J Math Chem (2010) 47:430–445
DOI 10.1007/s10910-009-9581-x

ORIGINAL PAPER

Computational modelling of amperometric biosensors in the case of substrate and product inhibition

Dainius Šimelevičius · Romas Baronas

Received: 3 June 2009 / Accepted: 23 July 2009 / Published online: 12 August 2009

Abstract In this paper the response of an amperometric biosensor at mixed enzyme kinetics and diffusion limitations is modelled in the case of the substrate and the product inhibition. The model is based on non-stationary reaction–diffusion equations containing a non-linear term related to non-Michaelis–Menten kinetics of an enzymatic reaction. A numerical simulation was carried out using a finite difference technique. The complex enzyme kinetics produced different calibration curves for the response at the transition and the steady-state. The biosensor operation is analysed with a special emphasis to the conditions at which the biosensor response change shows a maximal value. The dependence of the biosensor sensitivity on the biosensor configuration is also investigated. Results of the simulation are compared with known analytical results and with previously conducted researches on the biosensors.

Keywords Modelling · Simulation · Reaction–diffusion · Biosensor · Inhibition

1 Introduction

Biosensors are analytical devices incorporating a biological material, usually an enzyme, and a physicochemical transducer converting a biochemical recognition reaction into a measurable effect [1–3]. Amperometric biosensors measure the changes in the output current on the working electrode due to the direct oxidation or reduction of products of the biochemical reaction. The amperometric response is usually proportional to the concentration of an analyte (substrate) in a buffer solution. Amperometric biosensors are known to be reliable, cheap and highly sensitive for environment monitoring, food analysis, clinical diagnostics, drug analysis and some other purposes [4–7].

D. Šimelevičius (✉) · R. Baronas
Faculty of Mathematics and Informatics, Vilnius University, Naugarduko 24, 03225 Vilnius, Lithuania
e-mail: dainius.simelevicius@mif.vu.lt

Usually biosensors operate following the Michaelis–Menten kinetics scheme [2,3],

$$\mathrm{E} + \mathrm{S} \underset{k_{-1}}{\overset{k_1}{\rightleftharpoons}} \mathrm{ES} \xrightarrow{k_2} \mathrm{E} + \mathrm{P}, \tag{1}$$

where E is the enzyme, S is the substrate, ES is the enzyme and substrate complex, and P is the reaction product, k_i is the reaction rate constant, $i = -1, 1, 2$. However, very often the kinetics of enzyme-catalysed reactions is much more complex. An inhibition, an activation, an allostery and other types of non-Michaelis–Menten kinetics are known for the diversity of enzymes [8–12].

The inhibition is a process when a substance (inhibitor) diminishes the rate of a biochemical reaction [10]. In enzyme-catalysed reactions, the inhibitor frequently acts by binding to the enzyme. In this paper, a specific case of the non-Michaelis–Menten behaviour is investigated. It is the case when the enzyme-substrate complex ES interacts with one more substrate molecule producing a non-active complex ESS (the substrate inhibition) as follows:

$$\mathrm{ES} + \mathrm{S} \underset{k_{-3}}{\overset{k_3}{\rightleftharpoons}} \mathrm{ESS}. \tag{2}$$

In addition, an enzyme molecule interacts with the product molecule producing another non-active complex EP (the product inhibition),

$$\mathrm{E} + \mathrm{P} \underset{k_{-4}}{\overset{k_4}{\rightleftharpoons}} \mathrm{EP}. \tag{3}$$

The understanding of the kinetic peculiarities of the biosensors is of crucial importance for their design. To improve the productivity as well as the efficiency of the biosensor design, a model of the biosensor should be build [13,14]. Starting from the seventies various mathematical models have been widely used as important tools to study and optimize analytical characteristics of actual biosensors [15–18]. A comprehensive review on the modelling of the amperometric biosensors has been presented by Schulmeister [19]. Actual biosensors with the substrate as well as the product inhibition have been already modelled at various, usually steady-state, conditions [20–26]. The amperometric biosensors utilizing the enzyme with only the substrate inhibition has been recently modelled at the external diffusion limitation and the steady-state [12] as well as the transition conditions [27,28]. At the substrate concentration comparable to the Michaelis–Menten constant, the response change showed a maximal value [27].

This paper presents the results of non-stationary biosensor modelling at mixed enzyme kinetics, the external and the internal diffusion limitations with both kinds of the inhibition: the substrate and the product. The biosensor operation is numerically analysed with a special emphasis to the conditions at which the biosensor response change shows a maximal value. By changing physical as well as kinetic parameters the peak of the biosensor response was achieved at a wide range of the substrate concentrations. A numerical simulation has been carried out using a finite difference technique [29,30].

2 Mathematical model

The amperometric biosensor is considered as an electrode and a relatively thin layer of an enzyme (enzyme membrane) applied onto the electrode surface. The model involves three regions: the enzyme layer where the enzymatic reaction as well as the mass transport by diffusion takes place, a diffusion limiting region where only the mass transport by diffusion takes place and a convective region where the analyte concentration is maintained constant. Assuming the symmetrical geometry of the electrode and a homogeneous distribution of the immobilized enzyme in the enzyme membrane, the mathematical model of the biosensor action can be defined in a one-dimensional-in-space domain [19].

2.1 Governing equations

The governing equations for a chemical reaction network can be formulated by the law of mass action [1,18]. Coupling the enzyme-catalysed reaction in the enzyme layer with the one-dimensional-in-space diffusion, described by Fick's law, leads to the following equations of the reaction–diffusion type ($t > 0$):

$$\frac{\partial s_e}{\partial t} = D_{s_e}\frac{\partial^2 s_e}{\partial x^2} - k_1 e_e s_e + k_{-1} e_{es} - k_3 e_{es} s_e + k_{-3} e_{ess}, \tag{4a}$$

$$\frac{\partial p_e}{\partial t} = D_{p_e}\frac{\partial^2 p_e}{\partial x^2} + k_2 e_{es} - k_4 e_e p_e + k_{-4} e_{ep}, \tag{4b}$$

$$\frac{\partial e_e}{\partial t} = -k_1 e_e s_e + k_{-1}\, e_{es} + k_2 e_{es} - k_4 e_e p_e + k_{-4} e_{ep}, \tag{4c}$$

$$\frac{\partial e_{es}}{\partial t} = k_1 e_e s_e - k_{-1} e_{es} - k_2 e_{es} - k_3 e_{es} s_e + k_{-3} e_{ess}, \tag{4d}$$

$$\frac{\partial e_{ess}}{\partial t} = k_3 e_{es} s_e - k_{-3} e_{ess}, \tag{4e}$$

$$\frac{\partial e_{ep}}{\partial t} = k_4 e_e p_e - k_{-4} e_{ep}, \quad 0 < x < d_e, \tag{4f}$$

where x and t stand for space and time, respectively, $s_e(x,t)$, $p_e(x,t)$, $e_e(x,t)$, $e_{es}(x,t)$, $e_{ess}(x,t)$ and $e_{ep}(x,t)$ are the molar concentrations of the substrate S, the product P, the enzyme E, the ES complex, the ESS complex and the EP complex, respectively, d_e is the thickness of the enzyme layer, D_{s_e} and D_{p_e} are the diffusion coefficients of the substrate and the reaction product, respectively. The enzyme and the formed ES, ESS and EP complexes are immobilized, and therefore there are no diffusion terms in the corresponding equations.

Outside the enzyme layer only the mass transport by diffusion of the substrate and the product takes place. We assume that the external mass transport obeys a finite diffusion regime,

$$\frac{\partial s_d}{\partial t} = D_{s_d}\frac{\partial^2 s_d}{\partial x^2}, \tag{5a}$$

$$\frac{\partial p_d}{\partial t} = D_{p_d} \frac{\partial^2 p_d}{\partial x^2}, \quad d_e < x < d_e + d_d, \quad t > 0, \tag{5b}$$

where $s_d(x,t)$ and $p_d(x,t)$ stand for concentrations of the substrate and the product in the diffusion layer, d_d is the thickness of the external diffusion layer, D_{s_d} and D_{p_d} are the diffusion coefficients.

2.2 Initial and boundary conditions

Let $x = 0$ represent the electrode surface, $x = d_e$ is the boundary between the enzyme and the diffusion layers, and $x = d_e + d_d$ is the boundary between the diffusion layer and the bulk solution. The biosensor operation starts when some substrate appears in the bulk solution ($t = 0$),

$$s_e(x,0) = 0, \quad p_e(x,0) = 0, \quad 0 \le x \le d_e, \tag{6a}$$

$$s_d(x,0) = 0, \quad p_d(x,0) = 0, \quad d_e \le x < d_e + d_d, \tag{6b}$$

$$s_d(d_e + d_d, 0) = s_0, \quad p_d(d_e + d_d, 0) = 0, \tag{6c}$$

$$e_e(x,0) = e_0, \quad e_{es}(x,0) = 0, \quad e_{ess}(x,0) = 0, \quad e_p(x,0) = 0, \quad 0 < x < d_e, \tag{6d}$$

where s_0 is the concentration of the analyte (substrate) in the bulk solution, e_0 is the enzyme concentration.

Due to the electrode polarization concentration of the reaction product at the electrode surface ($x = 0$) is permanently reduced to zero [19],

$$p_e(0,t) = 0. \tag{7}$$

Since the substrate is not ionized, the substrate concentration flux on the electrode surface equals zero,

$$D_{s_e} \left. \frac{\partial s_e}{\partial x} \right|_{x=0} = 0. \tag{8}$$

The external diffusion layer ($d_e < x < d_e + d_d$) is treated as the Nernst diffusion layer [29]. According to the Nernst approach the layer of the thickness d_d remains unchanged with time. It is also assumed that away from it the solution is a uniform in the concentration ($t > 0$),

$$s_d(d_e + d_d, t) = s_0, \tag{9a}$$

$$p_d(d_e + d_d, t) = 0. \tag{9b}$$

On the boundary between two regions having different diffusivities, the matching conditions have to be defined ($t > 0$),

$$D_{s_e}\left.\frac{\partial s_e}{\partial x}\right|_{x=d_e} = D_{s_d}\left.\frac{\partial s_d}{\partial x}\right|_{x=d_e}, \quad s_e(d_e,t) = s_d(d_e,t), \tag{10a}$$

$$D_{p_e}\left.\frac{\partial p_e}{\partial x}\right|_{x=d_e} = D_{p_d}\left.\frac{\partial p_d}{\partial x}\right|_{x=d_e}, \quad p_e(d_e,t) = p_d(d_e,t)\,. \tag{10b}$$

According to these conditions, the substrate and the product concentration fluxes through the external diffusion layer are equal to the corresponding fluxes entering the surface of the enzyme layer. The concentrations of the substrate as well as the product from both layers are equal on the boundary between these layers.

2.3 Quasi-steady-state approximation

Some reactions in the network (1–3) are very fast, while others are considerably slower [2,3]. The large difference of timescales in the reaction network creates difficulties for simulating the temporal evolution of the network and for understanding the basic principles of its operation. To sidestep these problems, the quasi-steady-state approximation (QSSA) is often applied [31,32],

$$\frac{\partial e_e}{\partial t} \approx \frac{\partial e_{es}}{\partial t} \approx \frac{\partial e_{ess}}{\partial t} \approx \frac{\partial e_{ep}}{\partial t} \approx 0\,. \tag{11}$$

Assuming the QSSA leads to a reduction in the dimension of the system (4),

$$\frac{\partial s_e}{\partial t} = D_{s_e}\frac{\partial^2 s_e}{\partial x^2} - \frac{k_2(e_e + e_{es} + e_{ess} + e_{ep})s_e}{\frac{k_{-1}+k_2}{k_1}\left(1 + p_e/\frac{k_{-4}}{k_4}\right) + s_e\left(1 + s_e/\frac{k_{-3}}{k_3}\right)}, \tag{12a}$$

$$\frac{\partial p_e}{\partial t} = D_{p_e}\frac{\partial^2 p_e}{\partial x^2} + \frac{k_2(e_e + e_{es} + e_{ess} + e_{ep})s_e}{\frac{k_{-1}+k_2}{k_1}\left(1 + p_e/\frac{k_{-4}}{k_4}\right) + s_e\left(1 + s_e/\frac{k_{-3}}{k_3}\right)}\,. \tag{12b}$$

The total sum e_0 of the concentrations of all the enzyme forms is assumed to be constant in the entire enzyme layer, $e_0 = e_e + e_{es} + e_{ess} + e_{ep}$.

In order to reduce the number of the main governing parameters of the mathematical model, the following parameters are introduced:

$$V_{\max} = k_2 e_0 = k_2(e_e + e_{es} + e_{ess} + e_{ep}), \tag{13a}$$

$$k_M = \frac{k_{-1} + k_2}{k_1}, \quad k_s = \frac{k_{-3}}{k_3}, \quad k_p = \frac{k_{-4}}{k_4}, \tag{13b}$$

where $V_{\max}$ is the maximal enzymatic rate, k_M is the Michaelis–Menten constant, k_s is the substrate inhibition rate, and k_p is the product inhibition rate [1,2,31].

Finally, the governing equations (4) at the QSSA reduce to the following equations ($t > 0$):

$$\frac{\partial s_e}{\partial t} = D_{s_e}\frac{\partial^2 s_e}{\partial x^2} - v(s_e, p_e), \tag{14a}$$

$$\frac{\partial p_e}{\partial t} = D_{p_e} \frac{\partial^2 p_e}{\partial x^2} + v(s_e, p_e), \quad 0 < x < d_e, \tag{14b}$$

where $v(s_e, p_e)$ is the quasi-steady-state reaction rate,

$$v(s_e, p_e) = \frac{V_{\max} s_e}{k_M \left(1 + p_e/k_p\right) + s_e \left(1 + s_e/k_s\right)}. \tag{15}$$

In the case of the Michaelis–Menten kinetics, the condition for the QSSA to be valid is $e_0 \ll s_0 + k_M$ [32,33].

2.4 Characteristics of the biosensor response

The electric current is measured as a response of a biosensor in a physical experiment. The current depends on a flux of reaction product at an electrode surface. Thus the density i of the current at time t is proportional to the gradient of the product at the electrode surface, i.e. at the border $x = 0$, as described by Faraday's law,

$$i(t) = n_e F D_{p_e} \left.\frac{\partial p_e}{\partial x}\right|_{x=0}, \tag{16}$$

where n_e is a number of electrons involved in the electrochemical reaction, and F is Faraday's constant ($F = 96486\,\mathrm{C/mol}$) [2,19].

We assume that the system (5–10), (14) approaches a steady-state as $t \to \infty$,

$$i_{st} = \lim_{t \to \infty} i(t), \tag{17}$$

where i_{st} is assumed as the density of the steady-state biosensor current.

The sensitivity is also one of the most important characteristics of the biosensors. The biosensor sensitivity is usually expressed as the gradient of the biosensor current with respect to the concentration s_0 of the substrate in the bulk. Since the biosensor current as well as the substrate concentration varies even in orders of magnitude, a dimensionless expression of the sensitivity is preferable [2,34]. Two kinds of the dimensionless biosensor sensitivity have been investigated in this work. The steady-state current is used in the case of the first kind, while the maximal current is used for the second kind,

$$B_{st}(s_0) = \frac{\mathrm{d}i_{st}(s_0)}{\mathrm{d}s_0} \times \frac{s_0}{i_{st}(s_0)}, \tag{18a}$$

$$B_{\max}(s_0) = \frac{\mathrm{d}i_{\max}(s_0)}{\mathrm{d}s_0} \times \frac{s_0}{i_{\max}(s_0)}, \tag{18b}$$

where B_{st} and $B_{\max}$ stand for the dimensionless sensitivities of the amperometric biosensor, $i_{st}(s_0)$ is the density of the steady-state biosensor current calculated at the substrate concentration s_0, and $i_{\max}(s_0)$ is the maximal value of the density of the biosensor current calculated at the concentration s_0.

3 Numerical simulation

Because of non-linearity of the initial boundary value problem (5–10), (14) no analytical solutions are possible [16,19,29]. Hence the numerical simulation of the biosensor response was used. The simulation was carried out using the finite difference technique [29,30]. An implicit finite difference scheme was built on a uniform discrete grid with 200 points in space direction [11,35,36]. The simulator has been programmed by the authors in C++ language [37].

In the numerical simulation, the biosensor response time was assumed as the time when the change of the biosensor current over time remains very small during a relatively long term. A special dimensionless decay rate ε was used,

$$t_r = \min_{i(t)>0} \left\{ t : \frac{t}{i(t)} \left| \frac{\mathrm{d}i(t)}{\mathrm{d}t} \right| < \varepsilon \right\}, \quad i(t_r) \approx i_{st}, \tag{19}$$

where t_r is the biosensor response time. The decay rate value $\varepsilon = 10^{-3}$ was used in the calculations.

The mathematical model and the numerical solution have been validated using known analytical solution for a two layer model of the amperometric biosensor [19]. When solving the problem analytically, a few assumptions and model simplifications have to be introduced [34]. First of all it is considered that neither substrate nor product inhibition is observed during the biosensor operation (i. e., $k_s \to \infty$, $k_p \to \infty$). This assumption simplifies the expression of the general reaction rate (15) as follows:

$$v(s_e, p_e) \approx \frac{V_{\max} s_e}{k_M + s_e}. \tag{20}$$

Assuming (20), the initial boundary value problem (5–10), (14) can be solved analytically in the cases when the reaction function (15) approaches to a linear function [19]. At relatively low concentrations of the substrate when $s_0 \ll k_M$, the reaction rate v takes the following linear form:

$$v(s_e, p_e) \approx \frac{V_{\max} s_e}{k_M}. \tag{21}$$

Assuming (21), the density i_{st} of the steady-state current can be expressed as follows [19]:

$$i_{st} = n_e F D_{p_e} s_0 \frac{1}{d_e + d_d} \left(d_e + d_d \times \frac{D_{s_d} - \Phi D_{s_e} \sinh\Phi/\cosh\Phi}{D_{s_d} + \Phi D_{s_e}(d_d/d_e)\sinh\Phi/\cosh\Phi} \right) \times \left(\frac{\Phi D_{s_e} d_d}{d_e} \times \frac{\sinh\Phi}{\cosh\Phi} + \frac{D_{s_e} D_{p_d}}{D_{p_e}} \left(1 - \frac{1}{\cosh\Phi} \right) \right) / (D_{p_d} d_e + D_{p_e} d_d), \tag{22}$$

where Φ^2 is the diffusion modulus which was introduced in (26).

In all the numerical experiments the following values were kept constant:

$$D_{s_e} = D_{p_e} = 100\,\mu\text{m}^2/\text{s}, \quad D_{s_d} = 2D_{s_e}, \quad D_{p_d} = 2D_{p_e},$$
$$k_M = 0.01\ \text{M}, \quad d_e = 10\,\mu\text{m}, \quad d_d = 300\,\mu\text{m}, \quad n_e = 1. \tag{23}$$

The numerical solution of the model (5–10), (14) was compared with the analytical solution (22) at $k_s = 10^4\text{M}$, $k_p = 10^4\text{M}$ and $s_0 = 10^{-4}\text{M} = 0.01k_M$. The relative difference between the numerical and analytical solutions was less than 0.04%.

4 Dimensionless model

In order to define the main governing parameters of the mathematical model, the dimensionless mathematical model has been derived.

For simplicity, the concentrations s and p of the substrate and the product, respectively, can be defined in entire domain $x \in [0, d_e + d_d]$ as follows ($t \geq 0$):

$$s = \begin{cases} s_e, & 0 \leq x \leq d_e, \\ s_d, & d_e < x \leq d_e + d_d \end{cases} \tag{24a}$$

$$p = \begin{cases} p_e, & 0 \leq x \leq d_e, \\ p_d, & d_e < x \leq d_e + d_d. \end{cases} \tag{24b}$$

Both concentration functions (s and p) are continuous in the entire domain $x \in [0, d_e + d_d]$. Table 1 presents all the dimensionless parameters of the model.

The governing equations (14) in dimensionless coordinates are expressed as follows:

$$\frac{\partial S}{\partial T} = \frac{\partial^2 S}{\partial X^2} - \Phi^2 \frac{S}{\left(1 + P/K_p\right) + S\left(1 + S/K_s\right)}, \tag{25a}$$

$$\frac{\partial P}{\partial T} = \frac{D_{p_e}}{D_{s_e}} \frac{\partial^2 P}{\partial X^2} + \Phi^2 \frac{S}{\left(1 + P/K_p\right) + S\left(1 + S/K_s\right)}, \tag{25b}$$

Table 1 Dimensional and dimensionless parameters

Parameter	Dimensional	Dimensionless
Time	t, s	$T = tD_{s_e}/d_e^2$
Membrane thickness	d_e, cm	$\delta_e = d_e/d_e = 1$
Diffusion layer thickness	d_d, cm	$\delta_d = d_d/d_e$
Distance from electrode	x, cm	$X = x/d_e$
Substrate concentration	s, M	$S = s/k_M$, $S_0 = s_0/k_M$
Product concentration	p, M	$P = p/k_M$
Michaelis–Menten constant	k_M, M	$K_M = k_M/k_M = 1$
Substrate inhibition constant	k_s, M	$K_s = k_s/k_M$
Product inhibition constant	k_p, M	$K_p = k_p/k_M$
Current density	i, A cm^{-2}	$I = id_e/(n_eFD_{p_e}k_M)$

where

$$\Phi^2 = \frac{V_{\max} d_e^2}{D_{s_e} k_M}, \quad 0 < X < 1, \quad T > 0. \tag{26}$$

The governing equations (5) take the following form:

$$\frac{\partial S}{\partial T} = \frac{D_{s_d}}{D_{s_e}} \frac{\partial^2 S}{\partial X^2}, \tag{27a}$$

$$\frac{\partial P}{\partial T} = \frac{D_{p_d}}{D_{s_e}} \frac{\partial^2 P}{\partial X^2}, \quad 1 < X < 1 + \delta_d, \quad T > 0. \tag{27b}$$

The initial conditions (6) transform to the following conditions:

$$S(X, 0) = 0, \quad P(X, 0) = 0, \quad 0 \le X < 1 + \delta_d, \tag{28a}$$

$$S(1 + \delta_d, 0) = S_0, \quad P(1 + \delta_d, 0) = 0. \tag{28b}$$

The boundary conditions (7– 9) are converted to the following conditions ($T > 0$):

$$P(0, T) = 0, \tag{29a}$$

$$\left.\frac{\partial S}{\partial X}\right|_{X=0} = 0, \tag{29b}$$

$$S(1 + \delta_d, T) = S_0, \tag{29c}$$

$$P(1 + \delta_d, T) = 0. \tag{29d}$$

The matching conditions (10) take the following form:

$$\left.\frac{\partial S}{\partial X}\right|_{X=1^-} = \frac{D_{s_d}}{D_{s_e}} \left.\frac{\partial S}{\partial X}\right|_{X=1^+}, \tag{30a}$$

$$\frac{D_{p_e}}{D_{s_e}} \left.\frac{\partial P}{\partial X}\right|_{X=1^-} = \frac{D_{p_d}}{D_{s_e}} \left.\frac{\partial P}{\partial X}\right|_{X=1^+}. \tag{30b}$$

Assuming the same diffusivities for both species, the substrate and the product, the dimensionless model (25–30) contains only six following parameters: δ_d—the thickness of the diffusion layer, S_0—the concentration of the substrate in the bulk, K_s—the substrate inhibition constant, K_p—the product inhibition constant, Φ^2—the diffusion modulus, and $D_{\text{rel}} = D_{s_d}/D_{s_e} = D_{p_d}/D_{p_e}$—the ratio of the diffusivity in the diffusion layer to the diffusivity in the enzyme layer.

5 Results and discussion

Using numerical simulation, peculiarities of the biosensor action has been investigated at different values of the model parameters.

5.1 Dynamics of the biosensor response

Figure 1 shows the dynamics of the biosensor current. The biosensor action was simulated at different concentrations of the substrate ($1 \leq S_0 \leq 4$), a mean value of the diffusion modulus ($\Phi^2 = 1$) and moderate values of the substrate ($K_s = 0.1$) as well as the product ($K_p = 0.1$) inhibition constant.

At moderate substrate concentrations ($S_0 \leq 2.2$), the dimensionless biosensor current I is a monotonously increasing function of dimensionless time T. However, at relatively high substrate concentrations ($S_0 > 2.2$) the current I becomes a non-monotonous function of dimensionless time T. In the case of $S_0 = 4$, the maximal biosensor current is even about 4.3 times greater than the steady-state current. In all the cases of the non-monotony of the biosensor current ($S_0 > 2.2$), the maximal currents are practically the same.

Calculations show that the appearance of the maximal response value at high substrate concentrations is associated with the substrate inhibition. No non-monotony in the behaviour of the response of the amperometric biosensors is usually observed in the absence of the inhibition [1,9,16,19,27].

From the curves depicted in Fig. 1 one can also observe another important relationship: the steady-state current I_{st} is directly proportional to the substrate concentration S_0 at low substrate concentrations ($S_0 \leq 2.2$) and inversely proportional at high substrate concentrations. This effect is more thoroughly investigated in the next section.

5.2 Biosensor response vs. substrate concentration

The dependence of the maximal as well as the steady-state biosensor current on the substrate concentration was investigated at a constant substrate inhibition rate ($K_s = 0.1$) and different rates of the product inhibition. The biosensor response was simulated at relatively high product inhibition rate ($K_p = 0.01$), relatively low product inhibition

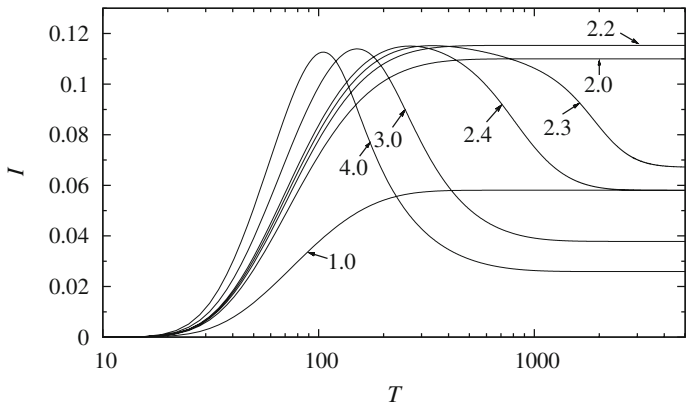

Fig. 1 Dynamics of the biosensor response at different values of the substrate concentration. Numbers on the curves show values of S_0, $\Phi^2 = 1$, $K_s = 0.1$, $K_p = 0.1$

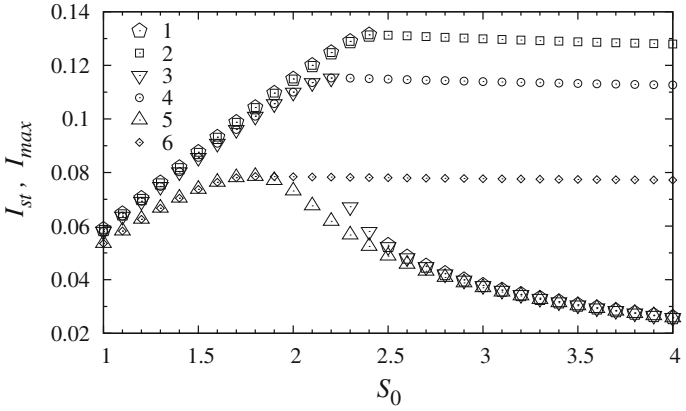

Fig. 2 The dependence of the maximal $I_{\max}$ (2, 4, 6) and the steady-state I_{st} (1, 3, 5) currents on the substrate concentration S_0 at three rates (K_p) of the product inhibition: ∞ (no inhibition) (1, 2), 0.1 (3, 4) and 0.01 (5, 6), $\Phi^2 = 1$, $K_s = 0.1$

rate ($K_p = 0.1$) and in the absence of the product inhibition ($K_p \to \infty$). In the case of no product inhibition, the reaction scheme (1–3) reduces to scheme (1), (2). Figure 2 shows calculated the maximal $I_{\max}$ and the steady-state I_{st} dimensionless biosensor currents versus the dimensionless substrate concentration S_0.

The results of the numerical simulation are depicted in Fig. 2.

When the product inhibition rate is relatively low ($K_p = 0.1$, curves 3 and 4) and is equal to the substrate inhibition rate ($K_p = K_s = 0.1$), the behaviour of the biosensor response is very similar to that which is observed in the case of absence of the product inhibition. As one can see in Fig. 2, a very sharp response change occurs when the substrate concentration S_0 is between 2.3 and 2.5. At these concentrations the steady-state and the maximal currents sharply diverge.

When the product inhibition rate is relatively high ($K_p = 0.01$), the sharp decrease in the response does not occur. The point where the maximal and the steady-state responses start to diverge is slightly shifted to the left ($S_0 = 1.9$).

The maximal responses are distinct for different rates of the product inhibition, especially at high substrate concentrations ($S_0 \geq 2.3$). Obvious correlation with the product inhibition rate is observed. However, the steady-state currents at $S_0 \geq 3$ are undistinguishable at different rates of the product inhibition.

5.3 Non-monotony of biosensor response

The effect of the divergence of the maximal and the steady-state biosensor currents was also observed in the case when only the substrate inhibition was considered [27]. This was explained by a multi-concentration generation that was also confirmed by the analytical solution of a simplified model with the external diffusion limitation at the steady-state conditions [12]. The biosensor response was then investigated only at moderate values of the diffusion modulus when the response change showed a

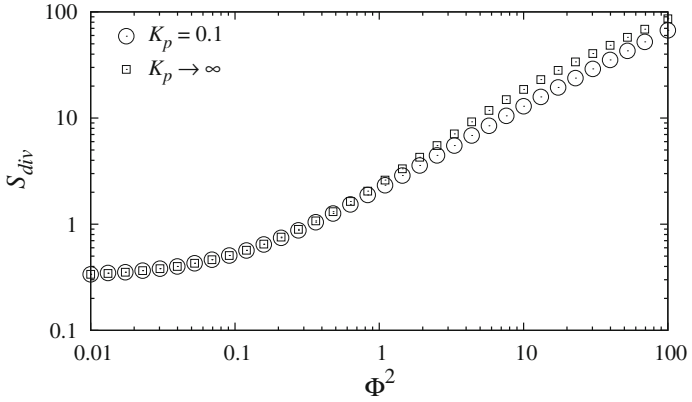

Fig. 3 The dependence of the substrate concentration S_{div} at which the response shows a maximal value on the diffusion modulus Φ^2 at two rates of the product inhibition K_p:∞ and 0.1, $K_s = 0.1$

maximal value at the substrate concentration comparable to the Michaelis–Menten constant k_M. Below the dependence of the divergence of the maximal and the steady-state biosensor currents on the substrate concentration is investigated in detail at a wide ranges of the diffusion modulus and the substrate as well as the product inhibition rate.

To investigate the effect of the diffusion modulus Φ^2 on the non-monotony of the biosensor response we introduce the minimal dimensionless substrate concentration S_{div} at which the response shows a maximal value,

$$S_{\text{div}}(\Phi^2, K_p, K_s) = \min\{S_0 : I_{\max}(\Phi^2, K_p, K_s, S_0) \neq I_{st}(\Phi^2, K_p, K_s, S_0)\}, \quad (31)$$

where $I_{\max}(\Phi^2, K_p, K_s, S_0)$ and $I_{st}(\Phi^2, K_p, K_s, S_0)$ are the dimensionless the maximal and the steady-state biosensor currents, respectively, calculated at appropriate values of Φ^2, K_p, K_s and S_0. At any substrate concentration S_0 less than S_{div}, the maximal and the steady-state currents are identical.

The results of the numerical simulation are depicted in Fig. 3. As one can see from the curves, the concentration S_{div} continuously and non-linearly increases with an increase in Φ^2. The concentration S_{div} is practically independent from the product inhibition rate K_p when the diffusion modulus is relatively low ($\Phi^2 \in [0.01, 0.1]$). When the diffusion modulus is relatively high ($\Phi^2 \in [1, 100]$), the product inhibition rate notably affects the S_{div}. A reason of this feature can be obtained from the structure of the governing equations (25). The influence of the biochemical reaction kinetics to whole process decreases when the diffusion modulus decreases. In other words, the concentration S_{div} notably depends on the the product inhibition rate K_p only if the biosensor response is controlled by the diffusion ($\Phi^2 \gg 1$). If the biosensor response is mainly determined by the enzyme kinetics ($\Phi^2 \ll 1$) then S_{div} is independent from the K_p. When the biosensor response is controlled by the diffusion, the value of S_{div} calculated in the case of no product inhibition ($K_p \to \infty$) is higher than that calculated in the case of the product inhibition ($K_p = 0.1$).

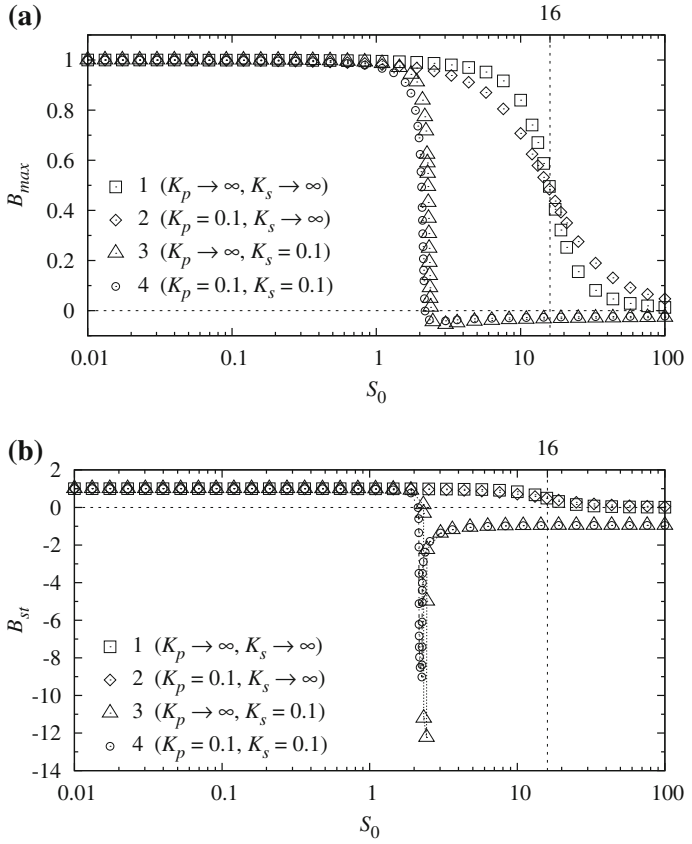

Fig. 4 The dependence of biosensor sensitivity $B_{\max}$ (**a**) as well as B_{st} (**b**) on the substrate concentration S_0

5.4 Biosensor sensitivity vs. substrate concentration

To investigate the dependence of the biosensor sensitivity on the substrate concentration, the biosensor response was simulated at two values of the substrate as well as the product inhibition rates and a wide range of substrate concentrations ($0.01 \leq S_0 \leq 100$). Having the simulated responses, both kinds of the biosensor dimensionless sensitivity, $B_{\max}$ and B_{st}, were calculated. Calculation results are depicted in Fig. 4.

Looking at Fig. 4 one can notice several distinctly different shapes of curves. Curves 1 and 2 corresponding to the biosensors with no substrate inhibition contain noticeably wider segments of the extremely high sensitivity ($B_{\max}$ and B_{st} equal approximately 1) than those corresponding to the biosensors with the substrate inhibition (curves 3 and 4). The substrate inhibition of the rate $K_s = 0.1$ leads to an approximately tenfold decrease in the upper boundary of the substrate concentrations at which the biosensor operation is highly sensitive. Both kinds of the sensitivity ($B_{\max}$ and B_{st}) of the biosensors with the substrate inhibition reach zero at the substrate concentration S_0 between 2.1 and 2.5, while the biosensors with no substrate inhibition show a fairly good (not

less than 0.5) sensitivity up to the concentration of $S_0 = 16$ when $B_{\max} \approx 0.5$. The effect of the product inhibition on the biosensor sensitivity ($B_{\max}$ as well as B_{st}) is rather low.

One can see in Fig. 4 that the sensitivity of the biosensors with the substrate inhibition can be even negative. A negative biosensor sensitivity means that the maximal (in the case of $B_{\max}$) or the steady-state (in the case of B_{st}) current decreases with an increase in the substrate concentration (see Fig. 2). In the case of the sensitivity based on the maximal response (Fig. 4a), negative values of $B_{\max}$ remains near zero ($0.02 < |B_{\max}| < 0.06$). The biosensors acting under the substrate inhibition of $K_s = 0.1$ and measuring only the maximal current are practically inapplicable to the prediction of the substrate concentrations higher than about $2k_M$ ($S_0 > 2,\ s_0 > 2k_M$).

When comparing the sensitivity B_{st} with the sensitivity $B_{\max}$ of the biosensors with the substrate inhibition, one can see noticeable difference in the shape of the curves presenting both kinds of the biosensor sensitivity. However, the difference is only observed at relatively high substrate concentrations ($S_0 > 2$) when both sensitivities, $B_{\max}$ and B_{st}, are negative.

The biosensors acting under the substrate inhibition and supporting the sensitivity B_{st} can be successfully applied to predict the substrate concentrations in the range where B_{st} is negative. Such intelligent biosensor should support two calibration curves, one for the concentrations at which the response is directly proportional to the substrate concentration, and the other for the concentrations at which the response is inversely proportional to the substrate concentration.

In the case with only the substrate inhibition (curve 3 in Fig. 4b), the biosensor sensitivity B_{st} reaches its negative peak at $S_0 = 2.4$ ($B_{st} = -12.2$). In the case with the substrate and the product inhibition (curve 4), the B_{st} reaches its minimal value at $S_0 = 2.3$ ($B_{st} = -9.0$). The points where the sensitivity curves show minimal values are the points where the biosensor steady-state response curves are the most steeply declined (see Fig. 5). At these points the substrate concentration can be very accurately predicted. At higher substrate concentrations up to $S_0 = 100$, the biosensor shows also very good values of sensitivity (B_{st} steadies at about -0.9, see Fig. 4b).

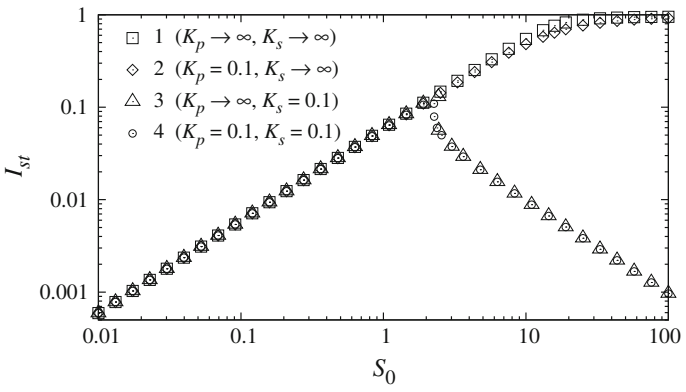

Fig. 5 The dependence of the steady-state dimensionless current I_{st} on the substrate concentration S_0

However regardless high absolute values of the sensitivity B_{st}, the biosensors with the substrate inhibition has a serious drawback. The measured steady-state current is not enough for the substrate concentration prediction. As one can clearly see in Fig. 5 that the steady-state current I_{st} is a non-monotonous function of the substrate concentration S_0. Because of this, an additional information is required to predict S_0 unambiguously. For instance, in addition to the steady-state current I_{st}, an intelligent biosensor could also take into consideration the maximal current $I_{\max}$. If $I_{st} < I_{\max}$ then the biosensor should use the calibration curve where I_{st} is inversely proportional to S_0. Otherwise, the concentration S_0 can be predicted under assumption of the proportionality of I_{st} to S_0. The ambiguity in the concentration prediction can be also solved if the substrate concentration S_0 is approximately known prior to the biosensor action.

After the examination of curves in Fig. 4 we can conclude that the measurement of the steady-state biosensor current is more useful than the measurement of the maximal current. In the case of the absence of the substrate inhibition, the measurement of the steady-state or maximal current makes no difference. However, in the case of the substrate inhibition, the measurement of steady-state current I_{st} could be more useful because of the possibility to measure higher substrate concentrations.

6 Conclusions

The mathematical model (5–10), (14) of the amperometric biosensor with the substrate and the product inhibition can be successfully used to investigate kinetic peculiarities of the biosensor response. The corresponding dimensionless mathematical model (25–30) can be used as a framework for numerical investigation of the impact of the model parameters on the biosensor response and to optimize the biosensor configuration.

The substrate inhibition leads to appearance of the maximal biosensor current different from the steady-state current (Figs. 1, 2 and 5). A complimentary product inhibition reduces the sharpness of the current drop (Fig. 2). The divergence of the maximal and the steady-state biosensor currents directly depends on the diffusion modulus Φ^2. The minimal dimensionless substrate concentration, at which the response shows a maximal value, is a monotonously increasing function of Φ^2 (Fig. 3).

At low substrate concentrations the steady-state as well as the maximal current can be equally used to predict the substrate concentration independent of the rate of the substrate as well as the product inhibition. In the case of the substrate inhibition, knowing both biosensor currents, the steady-state and the maximal, can be applied to significantly prolong the biosensor calibration curve. The effect of the product inhibition on the biosensor sensitivity is noticeably lower than that of the substrate inhibition.

Acknowledgments The authors express sincere gratitude to prof. Feliksas Ivanauskas and prof. Juozas Kulys for very useful discussions and their contribution to mathematical modelling of biosensors. This work was partially supported by Lithuanian State Science and Studies Foundation, project No. N-08007.

References

1. H. Gutfreund, *Kinetics for the Life Sciences* (Cambridge University Press, Cambridge, 1995)
2. F.W. Scheller, F. Schubert, *Biosensors* (Elsevier Science, Amsterdam, 1992)
3. A.P.F. Turner, I. Karube, G.S. Wilson, *Biosensors: Fundamentals and Applications* (Oxford University Press, USA, 1990)
4. J.F. Liang, Y.T. Li, V.C. Yang, J. Pharm. Sci. **89**(8), 979 (2000)
5. K.R. Rogers, Biosens. Bioelectron **10**(6–7), 533 (1995)
6. F.W. Scheller, F. Schubert, J. Fedrowitz, *Frontiers in Biosensorics II. Practical Applications*, vol. 2 (Birkhäuser, Basel, 1997)
7. D. Yu, B. Blankert, J.C. Vire, J.M. Kauffmann, Anal. Lett. **38**(11), 1687 (2005)
8. A. Chaubey, B.D. Malhotra, Biosens. Bioelectron. **17**(6–7), 441 (2002)
9. A. Cornish-Bowden, *Fundamentals of Enzyme Kinetics*, 3rd edn. (Portland Press, London, 2004)
10. N.C. of the International Union of Biochemistrys, Biochem. J. **213**(3), 561 (1983)
11. R. Baronas, F. Ivanauskas, J. Kulys, J. Math. Chem. **35**(3), 199 (2004)
12. J. Kulys, Nonlinear Anal. Model. Contr. **11**(4), 385 (2006)
13. J.R.D. Corcuera, R. Cavalieri, J. Powers, J. Tang, in *Proceedings of the 2004 ASAE/Csae Annual International Meeting* (American Society of Agricultural Engineers, Ottawa, Ontario, 2004), p. 47030
14. L.S. Ferreira, M.B.D. Souza, J.O. Trierweiler, O. Broxtermann, R.O.M. Folly, B. Hitzmann, Comp. Chem. Engng. **27**(8), 1165 (2003)
15. L.D. Mell, T. Maloy, Anal. Chem. **47**(2), 299 (1975)
16. J.P. Kernevez, *Enzyme Mathematics. Studies in Mathematics and its Applications* (Elsevier Science, Amsterdam, 1980)
17. J. Kulys, Anal. Lett. **14**(B6), 377 (1981)
18. P.N. Bartlett, R.G. Whitaker, J. Electroanal. Chem. **224**(1–2), 27 (1987)
19. T. Schulmeister, Selective Electrode Rev. **12**, 203 (1990)
20. S.K.C. Lin, C. Du, A. Koutinas, R. Wang, C. Webb, Biochem. Eng. J. **41**(2), 128 (2008)
21. S. Meric, O. Tunay, S.H. Ali, Environ. Technol. **23**(2), 163 (2002)
22. J. Mirón, M.P. González, J.A. Vázquez, L. Pastrana, M.A. Murado, Enzyme Microb. Technol. **34**(5), 513 (2004)
23. M. Mosche, H.J. Jordening, Water Res. **33**(11), 2545 (1999)
24. E.W.J. Niel, P.A.M. Claassen, A.J.M. Stams, Biotechnol. Bioeng. **81**(3), 255 (2002)
25. P. Shen, R. Larter, Biophys J. **67**(4), 1414 (1994)
26. H. Shinto, Y. Tashiro, M. Yamashita, G. Kobayashi, T. Sekiguchi, T. Hanai, Y. Kuriya, M. Okamoto, K. Sonomoto, J. Biotechnol. **131**(1), 45 (2007)
27. J. Kulys, R. Baronas, Sensors **6**(11), 1513 (2006)
28. D. Šimelevičius, R. Baronas, in *Information Technologies'2008—Proceedings of 14th International Conference on Information and Software Technologies*, ed. by A. Targamadzė, R. Butleris, R. Butkienė (Kaunas University of Technology, 2008), pp. 125–130
29. D. Britz, *Digital Simulation in Electrochemistry*, 3rd edn. (Springer, Berlin, 2005)
30. A.A. Samarskii, *The Theory of Difference Schemes* (Marcel Dekker, New York, 2001)
31. B. Li, Y. Shen, B. Li, J. Phys. Chem. A **112**(11), 2311 (2008)
32. L.A. Segel, M. Slemrod, SIAM Rev. **31**(3), 446 (1989)
33. A. Ciliberto, F. Capuani, J.J. Tyson, PLoS Comput. Biol. **3**(3), e45 (2007)
34. R. Baronas, J. Kulys, Sensors **8**(8), 4845 (2008)
35. R. Baronas, J. Kulys, F. Ivanauskas, J. Math. Chem. **39**(2), 345 (2006)
36. R. Baronas, F. Ivanauskas, J. Kulys, J. Math. Chem. **42**(3), 321 (2007)
37. W.H. Press, B.P.F.S.A. Teukolsky, W.T. Vetterling, *Numerical Recipes in C++: The Art of Scientific Computing*, 3rd edn. (Cambridge University Press, Cambridge, 2002)